Helsinki University of Technology, Laboratory of Paper and Printing Technology
Reports, Series A25
Espoo 2006

USING SLIT RHEOMETRY IN CHARACTERISING COATING COLOUR FLOW IN THE BLADE COATING PROCESS

Natalia Egorova

Dissertation for the degree of Doctor of Science in Technology to be presented with due permission of the Department of Forest Products Technology for public examination and debate in Auditorium 216 at Helsinki University of Technology (Otakaari 4, Espoo, Finland) on the 19th of May, 2006, at 12 noon.

Helsinki University of Technology
Department of Forest Products Technology
Laboratory of Paper and Printing Technology

Teknillinen korkeakoulu
Puunjalostustekniikan osasto
Paperi- ja painatustekniikan laboratorio

Distribution:
Helsinki University of Technology
Department of Forest Products Technology
Laboratory of Paper and Printing Technology

P.O Box 6300
FIN-02015 HUT

ISBN 951-22-8050-7
ISSN 1237-6248

Picaset Oy
Helsinki 2006

ABSTRACT

The aim of the present work was to evaluate the suitability of SLIT rheometry for characterising the coating colour flow in paper coating. The detailed aims were to determine the mechanisms governing the flow through the SLIT; to find out what kind of information on the coating colour flow that can be obtained with the SLIT; and to evaluate the ability of the SLIT to predict the relationship between coat weight and blade pressure.

For this purpose, flows of Newtonian model fluids and coating colours were studied both with conventional capillary and SLIT geometries attached to a high-shear rheometer. Correlations with laboratory coating data were determined for both geometries.

It was found that the flow through the SLIT does not attain a fully developed velocity profile and is unstable along the whole length of the SLIT. The instability caused by entrance effects is present at the exit from the SLIT as residual entrance pressure.

The SLIT geometry was found to be more sensitive to differences in coating colour formulations and also able to differentiate between coating colours displaying similar flow behaviour in conventional capillary measurements.

In a laboratory trial, the differences in coating formulations reflected by the SLIT measurements were found to be in good correlation with the blade position required to achieve the target weights. Coating colours demonstrating greater flow resistance in SLIT measurements required a smaller blade distance to achieve the required coat weight.

PREFACE

This work was carried out in the Laboratory of Paper Technology of the Helsinki University of Technology during 1999-2004 as a part of the International Doctoral Programme in Pulp and Paper Science and Technology (PaPSaT). Financial support from the Technology Development Centre of Finland, TEKES, is gratefully acknowledged.

I would like to express my warmest thanks to Dr. Jaakko Laine who supervised my studies for his encouragement and support. I would also like to thank Professor Hannu Paulapuro for his ever-valuable comments and advice.

I am indebted to Esa Lehtinen and Juha Happonen for introducing me to the theory and practice of paper coating rheology. I am also grateful to Eero Hiltunen for his empathy and help in making this work possible for me.

Finally, I wish to express my gratitude to my loved ones just for being with me.

LIST OF ABBREVIATIONS AND SYMBOLS

ABBREVIATIONS

CMC	Carboxymethyl cellulose
CLC	Cylindrical Laboratory Coater
PSD	Particle size distribution
SG95	SupraGloss 95
SW80	SupraWhite 80
SPR	Supraprint
HC90	Hydrocarb 90
pph	parts per hundred
SDR	Slit Die Rheometer

MATHEMATICAL SYMBOLS

$\dot{\gamma}_{wall}$	Shear rate at the capillary wall
τ_{wall}	Shear stress at the capillary wall
η	Viscosity
P	Extrusion pressure
Q	Volumetric flow rate
R	Radius of the capillary
h	Height of the SLIT
w	Width of the SLIT
L	Length of the capillary/SLIT
ρ	Density
$\bar{v}$	Flow velocity

LIST OF PUBLICATIONS

I. **Mäkinen, M., Egorova, N., Happonen, J., Lehtinen, E., Laine, J.E.**, "Using slit viscometers to predict coating perfomance on high speed Coaters", Paper Technology, 42(9):30-34 (2001)

II. **Egorova, N., Laine. J.E., Paulapuro, H.,** "On capillary and SLIT die rheometry (Part I)", Nordic Pulp Paper Res. J. 18(4):441-445 (2003)

III. **Egorova, N., Laine, J. E., Paulapuro, H.,** "On capillary and SLIT die rheometry (Part II)", Nordic Pulp Paper Res. J. 19(2):208-212 (2004)

IV. **Egorova, N., Laine, J. E., Paulapuro, H., "**Influence of coating colour composition on the SLIT flow", *accepted to Paperi ja Puu*

V. **Egorova, N., Laine, J. E., Paulapuro, H.,** "Geometry of the SLIT and its effect on the correlation with the coating process", Nordic Pulp Paper Res. J. 21(1):99-104 (2006)

Author's contribution to the publications

The author has made a major contribution to the experimental plan, experimental work, and analysis of the results and composed publications II-V.

TABLE OF CONTENTS

1 INTRODUCTION

Paper is coated to improve its optical and printing properties. In the coating of paper, an aqueous suspension, called coating colour, is applied to one or both sides of the paper. After application of the required amount, the coating is dried and finished. In finishing, the coated paper achieves its smoothness and gloss potential. Coated paper has better surface strength and less dusting, better gloss and opacity and lower ink absorption than uncoated paper. Therefore, the quality of the coating and the runnability of the coating process are of great importance for the quality of the final product.

Coating colours

Coating colours are water-based dispersions of mineral pigments and different additives. Additives such as binders, flow modifiers, dispersing agents, lubricants and other substances are added to the pigment slurry to give the coating colour its desired properties. Pigments usually comprise 80-90% or even more, on a dry basis, of the coating colour. The high content of pigments makes the rheological properties of coating colours dependent on those of the pigment slurry, although binders and rheology modifiers can alter these effects somewhat /1/.

The rheological behaviour of coating colours is a manifestation of many factors. Coating pigments are usually non-spherical particles with distribution in size and shape. Numerous experiments demonstrated that physical properties of coating pigments, such as particle size /2-5/, shape /3, 4, 6/ and size distribution /3, 5, 6/ influence the rheology of coating colours.

Pigment particles are often charged and exhibit strong inter-particle interactions. Suspended particles interact via electrostatic, van der Waals, and dipole-dipole forces. Surface activity of pigment particles strongly correlates with rheological properties of coatings bringing up the rise of viscoelasticity in coating colours /2, 6-9/.

Polymer additives (binders, thickeners, etc.) may increase liquid phase viscosity, absorbing on the particle surface or causing bridge or depletion flocculation /9-12/.

During the coating process, the coating formulation experiences a wide range of shear stresses lasting from a few microseconds up to several minutes. Depending on the shear rate, time of shearing and their composition and concentration, the coating colours may show yield stress, apparent shear

thinning, time dependent thinning (thixotropy) and shear thickening (dilatancy). Dilatancy may arise at high shear rates. This is a highly undesirable effect for the runnability of coating process /1, 7, 13/, though some research has shown good runnability with dilatant coatings /14, 15/. Besides the above-mentioned rheological properties, coating colours are also viscoelastic, which means that they have some ability to store energy and exhibit normal forces when sheared /6, 7, 13/.

Coating process

The coating process can be divided into different phases: application of the coating colour onto the base paper and metering of the coating to desired coat weight. Among the variety of coating techniques, blade coating is still the most common for effective metering and good levelling (Fig. 1.1).

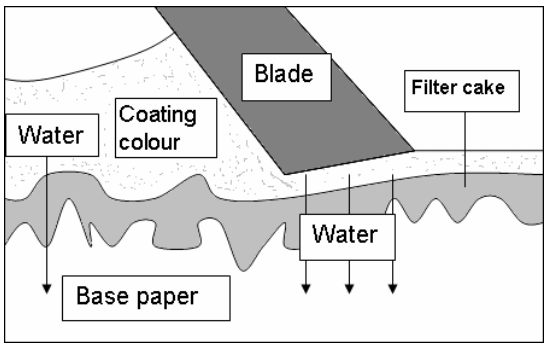

Fig. 1.1 Blade levelling process

In the blade levelling process, the load force of the blade is intended to control the coat weight. This force is in balance with the reaction force of the paper and backing roll, the impulse force originating from the coating colour hitting the blade, and the possible hydrodynamic lifting force, which may occur depending on the shape of the gap between the blade's tip and the paper.

In commercial blade coaters, coat weight control is achieved by adjusting the blade load force. Increased blade load force makes the paper more compressed and reduces its surface volume. This means that the coating colour entering the blade nip has fewer voids to fill. Therefore, increased blade pressure leads to reduced coat weight.

With a decrease in the blade loading force, a similar change in impulse and hydrodynamic forces automatically changes the reaction force of the paper. Therefore, the paper will have a larger void volume for the coating colour to

occupy. At high coat weights, where the blade loads are smaller, the impulse force starts to dominate the force balance /16, 17/.

In high angle mode when the rigid blade is used for metering purpose, changes of the blade angle affect the impuls force of the blade force balance. The lower the blade angle, the higher the impulce force acting on the blade since the excess coating colour back flow undergoes a severe directional change. Large impulse forces may disorient particles (especially platy ones) and create an impulse pressure effect in the region of the blade, which is likely to facilitate faster dewatering /18, 19/.

Low angle (0-15°) mode in case of the bent blades is traditionally used in slow machines at medium to heavy coat weights. In this case the blade nip is formed between the side of the blade and the paper, and is a lot longer than in the rigid blade case. Due to this the hydrodynamic force is a lot larger for a low-angle bent blade than for a rigid blade under otherwise similar conditions. Also the time spent by coating colour under the blade tip is longer in the low-angle mode than that in a high-angle one.
As modern paper machines are usually operated at high speeds (more than 1500 m/min), a technical challenge is to maintain high productivity with high quality. In blade coating, the average deformation rate at the blade nip is in the order of $10^{6}s^{-1}$, and the time spent by the coating colour under the blade is in the order of 10^{-5} sec /1, 7, 6, 13, 20/. It is important to maintain good runnability in coating, because the shear rate that the coating is subjected to under the blade increases with increasing machine speed.

Runnability

Good runnability is defined as coating without visual defects on the coated surface and a uniform coat weight. It also includes break-free operation of the coater, which is obtained by operating at a sufficiently low blade load with the coat weight in question. These aspects become more important when machine speed increases and coat weight decreases.

Runnability problems include build-up of coating on the blade called stalagmites, skips, streaks, spits and scratches on the coating and poor coat weight control. High blade pressure may lead to more frequent web breaks /21/.
There are several causes of runnability problems in the coating process (Fig. 1.2). The most important factors affecting high-speed coating include the rheological properties of the coating colour, the physical inter-particle packing characteristics of pigments, the presence of latex and the traditional

water retention aid (carboxymethyl cellulose, CMC) in the formulation, the dewatering properties of the coating colour, the base paper's porosity and absorbency, the base paper's stability and roughness, and the design of the coater head.

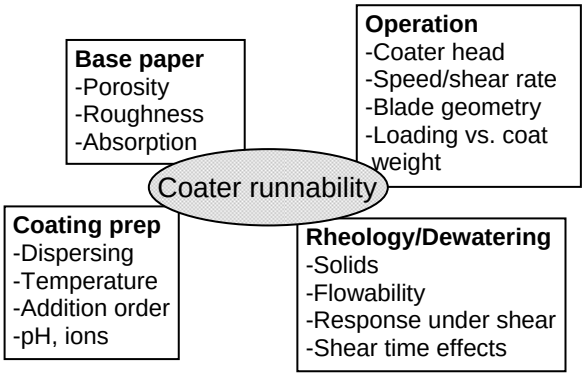

Fig. 1.2 Factors influencing runnability of coating colours

Under the pressure prevailing in the blade nip, the liquid phase migrates from the coating colour into the base paper (Fig. 1.1). It has been estimated that at a coater speed of 600 m/min, maximum pressure forces may reach 10^6-10^7 N/m^2 /19/. Therefore, the solids content of the coating colour rises almost instantaneously, which may lead to runnability problems. From this point of view, the absorption properties of the base paper are also important. A base paper with significant resistance to fluid phase intake may have an advantage over paper with a more open structure. The physical characteristics of pigments are also of importance for the pressure in dewatering. Closely packed platy particles (e.g. kaolin, talc) result in additional tortuosity in comparison with the use of blocky particles (e.g. calcium carbonate), restraining the passage of the liquid phase under pressure.

Pigment particles of different shapes have different hydrodynamic properties and behave in different ways when they move in liquid phase. Disk-shaped rotating particles in a suspension under shear are able to form a structure between two moving boundaries, especially at high solids content. These structures are responsible for generating large forces on the blade and the paper /22/. Platy kaolin particles will pass through the gap of the blade nip more easily if they are suitably pre-aligned /2, 6, 18, 19/. At very high flow rate changes, high-aspect-ratio particles are unable to retain their alignment with the flow. This results in a tendency for dilatancy and consequently poor runnability /18/.

Latex and CMC added to coating colour formulations as binders and water retention aids have been found to interact with pigment particles /23, 24/. This may lead to shear-induced aggregation with further distortion of coating quality.

Because of the high shear rate in the blade nip, the coating colour must have an optimum rheology. If viscosity is too low, splashing of the coating colour may occur; if viscosity is too high, it will cause runnability problems and poor quality of the coating layer /1, 7/.

The convergent geometry of the blade nip most likely makes the high-shear flow under the blade partly extensional /19/. Therefore, possible viscoelastic effects under the blade should not be ignored, since they may be responsible for the onset of coating non-uniformities and coating defects /25/.

Another runnability problem concerns coat weight control: either accepting non-uniform coat weight across the web, or using high blade pressure to achieve the target coat weight. To avoid web breaks, the blade pressure needed to reach the target coat weight should be minimised /21/.

As can be seen from the above, all the factors affecting the runnability of the coating process are strongly interrelated. However, the main factors influencing runnability are the solids content of the coating colour, its rheology and water retention /16/.

Predicting runnability by means of rheometry

There are no laboratory methods for assuring coater runnability, although various measurements of the rheological properties of the coating colour can help in evaluating runnability. First, the rheological behaviour of paper coating formulations is a key factor influencing runnability, water retention, and coating holdout. Understanding how to control coating rheology is critical for achieving good runnability and for optimum placement of the coating. Second, rheology is a powerful tool for characterizing the interactions between the different components of a paper coating formulation. It also serves as a quality control measurement.

Understanding the different types of information provided by rheological measurements can improve the design of new coating formulations.

Different types of rheometers exist for measurements of rheological properties of paper coatings.

A Brookfield type viscometer can provide some rheological information of the coating in the shear range from 10^{-1}-10^{3} sec^{-1}, which represents mixing, pumping, and storage. Rotational rheometers are able to give information in the range of 10^{-1}-10^{5} s^{-1} depending on the measuring geometry. The big advantage of the capillary viscometer is its ability to reach ultra-high shear rates (10^{6}-$2 \cdot 10^{6}$ s^{-1}). It is clear from the foregoing that realistic shear rate occurring under the blade can only be achieved with capillary rheometers.

Many researchers have tried to correlate the rheological behaviour of coating colours with blade coater performance /13, 20, 21, 26/. The flow behaviour of coating colours has been found to influence runnability, while also affecting porosity, gloss, brightness, opacity, i.e. the quality of coated and printed papers /1, 6, 7/.

Roper and Attal /21/ measured the viscosity of coating formulations from very low to very high shear rates using a combination of rheometers. They used rotational rheometers to collect low- and intermediate-shear data, and a capillary rheometer to collect high-shear data. High-shear viscosity appeared to be in good correlation with the blade pressure needed to achieve the target coat weight, provided that coating was performed with the run on the land of the blade and minimum blade wear.

Grankvist and Sandås /26/ studied the viscoelastic properties of coating colours at high shear rates also using a capillary rheometer. They concluded that this experimental technique may be one of the closest to the real coating situation. However, this conclusion contradicts other findings, which show that coating colours behave like viscoelastic materials only under small deformation rates and are inelastic at high deformations /27/. Triantafillopoulos also points out the inelastic behaviour of coating colours at high shear rates /7/.

The high-shear flow behaviour of coating colours has been commonly studied with capillary rheometers /13, 20, 21, 26, 28/. Slit rheometry is a comparatively new technique for studying the rheology of coating colours, although it has applications in other industries /28, 29/.

Ramthun et al. /30/ observed that measurements with slit geometry highlight differences in flow behaviour of coating colours in the cases where different binder systems, levels of solids content and latexes with different particle size are used in the coating colour formulation.

In research conducted by Tsuj et al. /31/, another type of slit die rheometer was found to be a good simulator of coating colour flow under the blade tip in actual coating. The rheometer provided accurate information on the high-shear properties of coating colours, which correlated well with coating colour runnability. Further, the entrance pressure data simulated the unsteady flow behaviour under the blade, reflecting the dynamic state of particle orientation under high shear rates, which also relates to runnability.

From the examples given above one can conclude that different rheology measurement techniques are good tools for predicting coating colour behaviour during coating. Nevertheless, there is no agreement among researchers concerning the most realistic rheology measurement technique for predicting the behaviour of coating colours.

Recently, Mäkinen et al. have introduced a novel slit measuring system (in the following referred to as SLIT) /32/. Unlike the previously studied slit systems, the geometry and dimensions of the new system were very close to those of the blade nip (Fig. 1.3). With capillary rheometers it is only possible to achieve realistic shear rates, whereas with the novel SLIT realistic shear rates (up to $3 \cdot 10^6 s^{-1}$), shearing times and flow velocities can be obtained. Therefore it can assumed that SLIT geometry of high shear rheometer would be advantageous in prediction of coating colours runnability in real coating process in comparison to conventional techniques widely used nowadays.

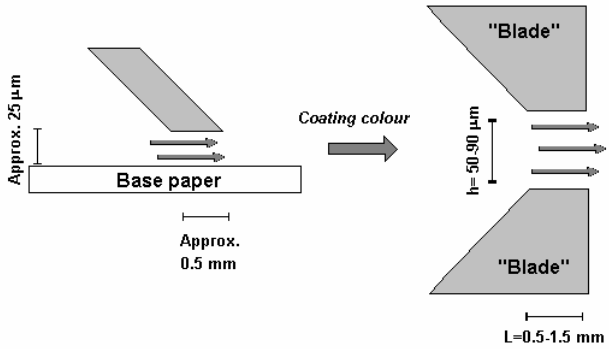

Fig. 1.3 Schematic diagram of the coater blade and SLIT measuring die.

2 THEORY

This chapter presents currently available information on the fundamentals of the flow through the capillary and SLIT.

2.1 Capillary rheometry

2.1.1 Principle of measurements

A capillary is a circular tube normally made of glass or stainless steel. In high-shear rheometers capillaries with a length of 30-70mm and a diameter of 0.4-0.7mm are normally used. Since capillary rheometry is widely used, the fundamentals of the flow are well known. High shear is achieved in capillary rheometers by applying external pressure to the measured sample. The extrusion pressure and flow rate through the capillary of known length and diameter are recorded. From the measured values of the flow rate and applied pressure, the shear rate (γ) and shear stress (τ) are calculated as follows:

$$\dot{\gamma}_{wall} = \frac{4Q}{\pi R^3} \qquad (2.1\text{-}1)$$

$$\tau_{wall} = \frac{pR}{2L} \qquad (2.1\text{-}2)$$

In these equations Q is the volumetric flow rate, p is the extrusion pressure and R and L the radius and length of the capillary, respectively.

Viscosity is defined according to the equation:

$$\eta = \frac{\tau_{wall}}{\dot{\gamma}_{wall}} \qquad (2.1\text{-}3)$$

Pressure profiles for Newtonian and non-Newtonian fluids

When Newtonian fluid is measured, part of the pressure applied to the sample (P_{meas}) dissipates in the form of kinetic energy, which is needed to accelerate a fluid from rest (P_{kin}). When fluid enters a capillary from a large reservoir, the velocity profile starts to develop and continues to change until it becomes fully developed. The length of the capillary required to reach a fully developed profile depends on the velocity of the fluid, the diameters of the capillary and reservoir, and the viscosity of the fluid. Therefore, another part of the applied pressure is lost due to the abrupt changes in the flow velocity profile at the entrance to the capillary and its further development in the die.

This pressure drop is referred to as the entrance pressure loss (P_{Nent}). The pressure drop within the capillary is entirely due to viscous dissipation (P_{visc}), and upon exit from the capillary the pressure becomes equal to the ambient pressure.

The total pressure difference between a point ahead of the measuring die and the exit of can be described by the following equation:

$$P_{meas} = P_{kin} + P_{Nent} + P_{visc} \qquad (2.1\text{-}4)$$

The pressure profile before and within the capillary is presented schematically in Fig. 2.1.

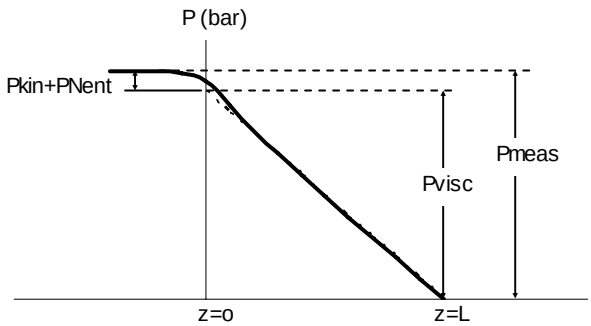

Fig. 2.1 Schematic diagram of the pressure distribution before and in the capillary (Newtonian fluid).

For non-Newtonian and viscoelastic fluids, such as polymers or coating colours, the energy dissipation becomes more complicated. First of all, one more component contributes to the entrance pressure drop: the pressure drop, which may be converted into elastic energy (P_{elast}). Because of the elastic properties of a fluid, the entrance pressure loss is much higher than that of Newtonian fluids /28, 33/. Above all, the elasticity of the fluid also affects the pressure at the exit from the capillary; the exit pressure (P_{exit}) becomes higher than the ambient one /28, 33, 34/. Thus, the pressure dissipation in the case of viscoelastic materials can be described by the following equation:

$$P_{meas} = P_{kin} + P_{Nent} + P_{elast} + P_{visc} + P_{exit} \qquad (2.1\text{-}5)$$

The pressure distribution would appear as shown in Fig. 2.2

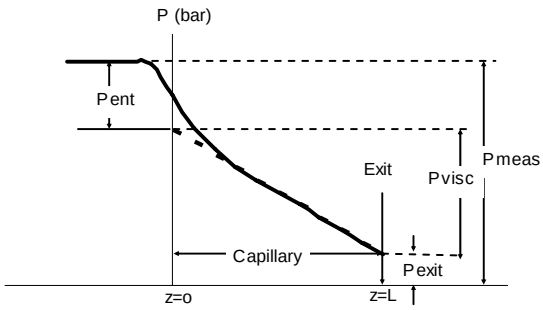

Fig. 2.2 Schematic diagram of the pressure distribution before and in the capillary (non-Newtonian/viscoelastic fluid). P_{ent} is a sum of P_{kin}, P_{Nent}, and P_{elast}.

It is necessary to know P_{visc} to calculate viscosity (see equations 2.1-1 – 2.1-3), but unfortunately it is impossible to measure it directly. Therefore, a number of corrections are used to calculate it from the measured pressure.

2.1.2 Corrections of the flow

Kinetic energy corrections

For rheometry at high shear rates, a "kinetic energy correction" is often needed, in which the viscous pressure drop is calculated by subtracting the pressure needed to accelerate the fluid from rest (P_{kin}) from the total pressure drop (P_{meas}). Energy losses due to this effect are proportional to the square of the velocity of the fluid entering the narrow orifice:

$$P_{kin}=m\rho\bar{v}^2 \qquad (2.1\text{-}6),$$

where ρ is the density of the fluid, $\bar{v}$ is flow velocity, and m is the kinetic energy correction coefficient (for capillaries m is equal to 1, for rectangular ducts it is about 0.8).

The correction is applied for Newtonian and non-Newtonian fluids.

Bagley correction for end effects

Viscoelastic fluids tested with a capillary rheometer demonstrate different flow curves for different dimensions of the capillaries. This is attributed to

the presence of the entrance and exit effects described above. In order to correct the measured pressure drop for the end effects, a correction called Bagley /35/ should be applied. The Bagley correction accounts both for the viscous and elastic components of the end pressure drop (components P_{Nent}, P_{elast}, and P_{exit} in Eq. 2.1-5) and is applied in the case of non-Newtonian fluids.

The end losses are determined experimentally for each studied material. This involves determination of the volumetric flow rate or shear rate versus the total applied pressure using capillaries of at least three different lengths but the same diameter. Then values of total applied pressure are read for each capillary length at a specific value of the flow rate or shear rate and plotted against length-to-diameter ratios. According to Bagley /35/, at a given flow rate/shear rate and tube diameter the end pressure drop is independent of the die length. Therefore, a typical Bagley plot depicts the total pressure drop versus the length-to-diameter ratio (aspect ratio), where points are situated linearly (Fig. 2.3). The curve obtained is extrapolated to its interception with the L/d axis, and the end pressure losses are read as intercepts on the P axis at L/d=0.

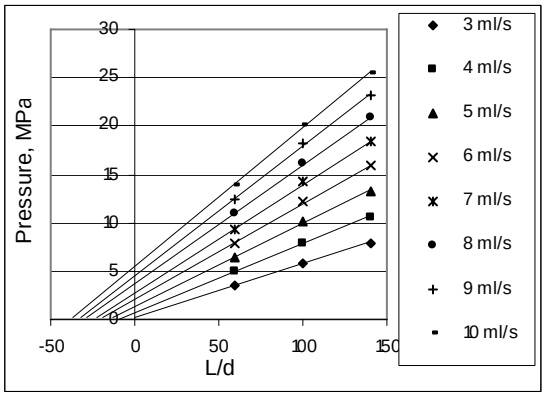

Fig. 2.3 Typical Bagley plot obtained from capillary measurements of calcium carbonate-based coating colour. Each straight line corresponds to a constant flow rate.

The kinetic energy and end losses are then subtracted from the measured pressure values and corrected viscosity values are calculated. After the corrections, the true viscosity of the measured fluid independent of the geometry of the capillary is obtained.

2.2 Introduction to slit rheometry

2.2.1 Principle of measurements

The principle of slit rheometry is the same as of capillary rheometry: the pressure- driven flow through the orifice. Nevertheless, the shape of the measurement channel is different. The SLIT die is designed to simulate the geometry of the blade nip of a commercial blade head. The entrance angle of the SLIT is 45°, the length of the orifice about 0.5 mm, and the height about 0.05mm (Fig. 1.3), which is close to the dimensions of the blade nip. With SLIT geometry it is possible to achieve not only realistic shear rates (up to $3 \cdot 10^6 s^{-1}$) but also shearing times and flow velocities.
As in a case of the capillary measurement, in the SLIT measurement flow rates and extrusion pressures are monitored and used for calculating the rheological parameters.

The equations for the flow through the rectangular die are applied to the SLIT flow rates and pressure in order to calculate shear rate (γ), shear stress (τ) and viscosity (η):

$$\dot{\gamma}_{wall} = \frac{6Q}{wh^2} \qquad (2.2\text{-}1)$$

$$\tau_{wall} = \frac{ph}{2L} \qquad (2.2\text{-}2)$$

$$\eta = \frac{\tau_{wall}}{\dot{\gamma}_{wall}} \qquad (2.2\text{-}3)$$

where Q is the volumetric flow rate; p is the extrusion pressure; and h and w the height and the width of the SLIT, respectively, and L is the SLIT length.

2.2.2 Corrections of the flow

Kinetic energy correction is applied to the slit results in the same way as in capillary measurements (See section 2.1.2).

As streamlines of the fluid contract in the SLIT, part of the applied pressure dissipates for the development of the flow profile. The Couette correction

suggests using the "effective length" instead of the physical length of the SLIT, thus compensating for this pressure loss:

$$L'=L+n \qquad (2.2\text{-}4),$$

where L is length of the capillary/SLIT, L' is the "effective length" of the capillary/SLIT, and n is the diameter/height of the capillary/slit correspondingly.

The Couette correction is insignificant if the length of the measuring channel is much greater that its diameter or height. This means that in capillary rheometry the Couette correction is negligible and can be omitted but should be used in SLIT rheometry.

Shear stress in the measuring die after kinetic and Couette corrections is transformed according to the following:

$$\tau=\frac{p_{meas}-p_{kin}}{2L'} \qquad (2.2\text{-}5)$$

2.2.3 Aims of the work

In the previous chapter, currently available information about the flow through the SLIT was presented. The slit rheometry has found applications in a number of industries, for instance in polymer processing, whereas the use of slit rheometry in coating research is of comparatively recent origin. For this reason, there is only very little information available concerning the use of slit rheometry for studying coating colours. This applies in particular to rheometry with a specific SLIT design.

According to several studies, SLIT rheometry provides higher values of viscosity than the conventional capillary method /32, 36, 37/. No clear explanation of this phenomenon has been given. Therefore, the following aims were set for the present study:

1. To determine the mechanisms governing the flow through the SLIT / and what factors affect the flow of coating colour through the SLIT
2. To find out what kind of information about the coating colour flow behaviour that can be obtained with the SLIT in comparison with the conventional capillary method

3. To evaluate the ability of the SLIT to predict the relationship between coat weight and blade pressure
4. To optimise the dimensions of the SLIT, aiming for a good compromise between prediction ability and ease of use.

3 EXPERIMENTAL

In the experimental part of this work, two model Newtonian fluids of standard viscosities were tested in order to compare the mechanisms governing the flow through the capillary and SLIT.

The coating colours were selected to resemble, in general, industrial coating colours used today. The pigments used in coating colour formulations differed in terms of particle shape and particle size distribution. The properties of the pigments and chemicals used for coating colour preparation are given in the following section.

3.1 Materials

Silicone fluids

Two siloxane oils (Algol Oy) with standard viscosities of 50 mPa·s and 100 mPa·s and densities of 0.9712 and 0.9693 kg/l, respectively, were used as model Newtonian fluids. The sensitivity of siloxane oils to temperature changes was checked in the temperature range 20-50°C. Standard values of viscosity (50 and 100 mPa·s) were obtained at 25°C.

Pigments

In different stages of the study, the following pigments were used for preparing coating colours: three grades of English kaolin (SupraGloss 95 (SG95), SupraWhite 80 (SW80), and Supraprint (SPR), IMERYS) and calcium carbonate (Hydrocarb 90 (HC90), OMYA).

Table 3-1 Pigment properties

	SG95	Supraprint [1)]	SW80	HC90
Shape factor	25-30	30-35	15-25	
Mass % of particles <2µm	92	92	80	90
Conc. % solids for 500 mPa·s [2)]	69.0	70.0	69.5	N/A
Conc. % solids for cap. visc. Consistent [3)]	59.5	60.0	61.3	68.0

[1)] Supraprint is engineered kaolin clay
[2)] Solids content for 500 mPa·s viscosity (Brookfield, 100 rpm)
[3)] Solids content for consistent capillary viscosity (ACAV-A2; capillary diameter 0.5 mm, length 50 mm)

Binders and thickeners

Sodium carboxymethyl cellulose (CMC) (Finnfix 10 (Molecular weight 63 000) and Finnfix 5 (Molecular weight 45 000), Noviant) was used as a thickening agent. Styrene-butadiene latex, Baystal 8110 (Eka Polymer Latex Oy) was used as a binder.

Coating colour formulations

Kaolin clays were received in dry form and dispersed in water with sodium polyacrylate salt (Polysalz) as a dispersing agent. For Supraprint 0.35 parts of dispersant per 100 parts of clay by weight (pph) and for other clays 0.30 pph of dispersant were used. Supraprint kaolin clay required a higher dose of dispersing agent to ensure optimum dispersion of the given engineered pigment /38/. Calcium carbonate was received as a slurry. For coating colour preparation 11 pph of latex and 1 pph of CMC were used in all formulations. The solids content of coating colours with high molecular weight was varied to make the capillary high-shear viscosity consistent for all pigments (Table 1). With low-molecular-weight CMC, the solids content of coating colours was kept on the level shown for each pigment in Table 1. The final pH was controlled with sodium hydroxide at the level of 8.

3.2 Methods

Rheological measurements

An Ubbelohde viscometer with a temperature control system was used for evaluating the effect of temperature on the viscosity of the model Newtonian fluids (siloxane oils). The viscometer is fitted inside a double wall glass cylinder for thermostating with a circulating thermostat. The flow time of the liquid is measured. A high-precision thermometer is attached for temperature measurement.

A schematic drawing of the viscometer setup is shown in Figure 3.1.

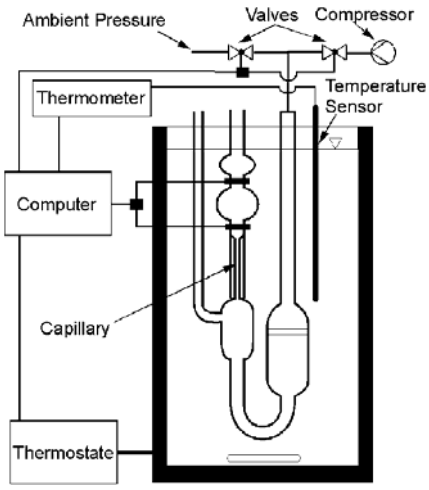

Fig. 3.1 Ubbelohder viscometer

A pressure-driven ultra high shear viscometer from ACA Systems Oy was used for high-rate measurements. The A2 model of the viscometer (Fig. 3.2) can be fitted with a conventional holder for a glass capillary, low shear rate capillary or a SLIT die attachment, which are interchangeable.

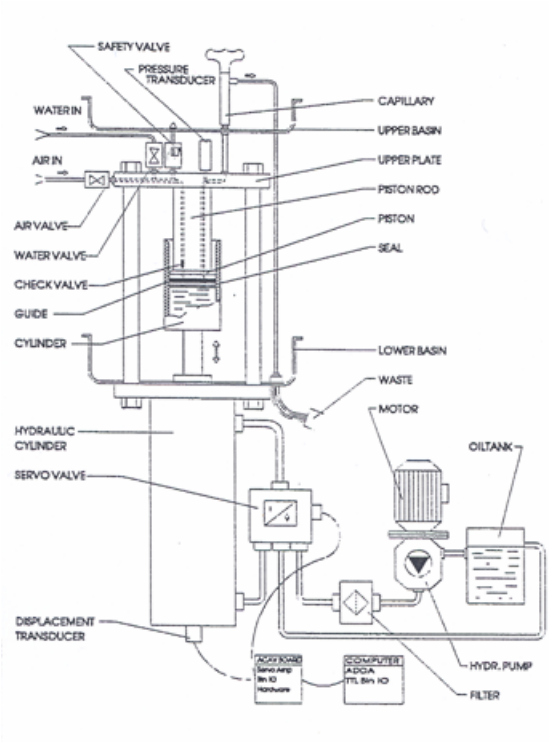

Fig. 3.2 ACAV-A2 Ultra High Shear Viscometer

The test sample is placed into the sample cylinder, which can be pressurised to the required pressure level up to 350 bar. The hydraulic piston moves the cylinder upwards, pushing the sample through the measuring die. The pressure transducer controls the extrusion pressure. The measured pressure and flow rate data are recorded by the computer software, provided that the exact dimensions of the measuring die allow the software to calculate the rheological parameters, such as shear rate, shear stress, viscosity.

Dimensions of capillaries and SLITs

Highly abrasive pigments cause abrasion of the capillary walls or at least smoothen the edges around the entrance, which may affect the measurements. A recommended procedure to avoid changes in the flow conditions is to calibrate the capillaries frequently enough. The dimensions of the capillaries are given in Table 3-2. The SLIT geometry is made of steel, which is diamond-coated to minimise wear of the measuring die. Still, the SLIT die was frequently calibrated in order to control its precise dimensions.

Table 3-2 Capillary dimensions (mm)

	Length	Diameter	L/d
Capill. № 1	30	0.5	60
Capill. № 2	50	0.5	100
Capill. № 3	70	0.5	140
Capill. № 4	50	0.4	125

According to the aims of the study, five height levels for the SLITs were chosen: 50, 60, 70, 80, and 90 micrometers. The height of the SLIT can be changed by varying the thickness of the metal film inserted between the two parts of the SLIT. The parts of the SLIT are assembled and screwed tight, thus creating a measuring channel of a certain height. The metal films of precise thickness were delivered by ACA Systems Oy.

The dimensions of the SLIT were estimated with high accuracy by means of a water calibration procedure. The SLIT height obtained once cannot be repeated for a second time without slight deviations. Therefore, in order to eliminate possible deviations in SLIT dimensions, all the experiments were designed to minimise the need for height changes. The gap of the SLIT was only changed after all test materials had been measured with a given SLIT height. Since the siloxane oils were tested before the coating colours, it was impossible to avoid changes in the gap when experiments with coating colours were started. Therefore, the SLIT heights used for measurement of siloxane fluids (Table 3-3) differ slightly from those used in measurements of coating colours (Table 3-4). However, the difference is insignificant for the results and conclusions derived.

Table 3-3 SLIT dimensions in experiments with siloxane oils (mm). (Paper II)

SLIT	Length	Width	Height 1	Height 2	Height 3	Height 4	Height 5
№ 1	0.5	10	0.0472	0.0561	0.0654	0.0838	0.0902
№ 2	1.0	10	0.0507	0.0587	0.0664	0.0857	0.0925
№ 3	1.5	10	0.0508	0.0585	0.0665	0.0855	0.0928

Table 3-4 SLIT dimensions (mm) and aspect ratios in experiments with coating colours. (Papers III, IV, V)

SLIT*)	Length	Height 1	*L/h*	Height 2	*L/h*	Height 3	*L/h*
№ 1	0.5	0.0506	9.9	0.0861	5.8	0.0905	5.5
№ 2	1.0	0.0440	22.7	0.0816	12.2	0.0905	11.0
№ 3	1.5	0.0501	29.9	0.0843	17.8	0.0914	16.4

*) All SLITs had a width of 10mm.

Coating trial

The coating trial was carried out in KCL (Finnish Pulp and Paper Research Institute) on a Cylindrical Laboratory Coater (CLC-6000). The base paper was a commercial LWC base paper with a grammage of 48 g/m^2. The paper was one-side coated from the inner side. Two target coat weights of 6 and 12 g/m^2 were used during the coating trial. Coating was performed at the machine speeds of 600, 900, and 1200 m/min.

4 RESULTS AND DISCUSSION

This chapter presents the results of the SLIT viscometry evaluation. Included are experiments based on capillary and SLIT measurements with model Newtonian fluids and coating colours, and results of laboratory coating trials.

4.1 Oils

4.1.1 Measurements with capillaries

The capillary viscosity of siloxane oils vs. shear rate is depicted in Fig. 4.1. The viscosity of both measured oils, corrected for kinetic energy losses, is independent of the dimensions of the capillaries.

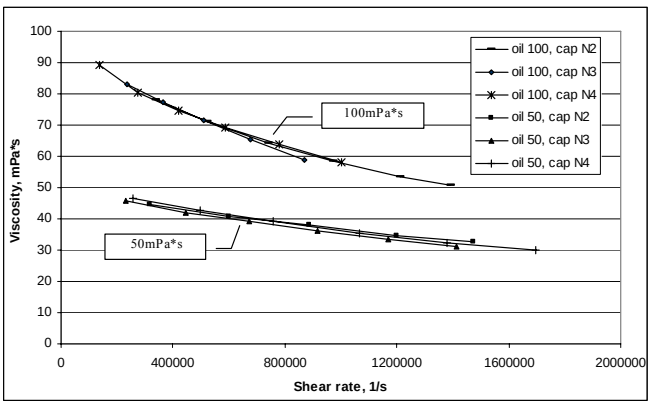

Fig. 4.1 High-shear viscosity of siloxane oils, 50 mPa·s and 100 mPa·s, measured with capillaries of different dimensions. Kinetic correction is applied

The capillaries used show values below the standard viscosity of oils, and the viscosity curves demonstrate a dependence of the shear rate, which is unexpected for Newtonian fluids.

The dependence of the oils' viscosity of temperature was checked in the Ubbelohder viscometer with a thermostat. The temperature in the thermostat was raised from 20°C to 50°C, and the viscosity of the oils was measured after each 5°C increase in temperature. The viscosity of both oils demonstrated a pronounced dependence of temperature (Fig. 4.2). A temperature rise by 30°C led to decrease in viscosity by 40%.

In high-shear capillary measurements, the initial temperature of samples was kept at 24°C and the temperature on exit from the measuring die was monitored. The temperature of measured oils on exit from the capillary increased by 12-20°C. The temperatures and viscosities of the sample obtained in high-shear-rate measurements are compared with those obtained in the Ubbelohde experiment in Fig. 4.2. The decrease in viscosity in the high-shear capillary measurements shows the same trend as in Ubbelohde measurements, although viscosity in the former case seems to be more sensitive to increased temperature.

The fact that the high-shear capillary viscosity of oils was lower than the standard values (50 and 100 mPa·s) and that the viscosity curves demonstrated pronounced shear-dependent behaviour (Fig. 4.1) was attributed to the effect of shear heating.

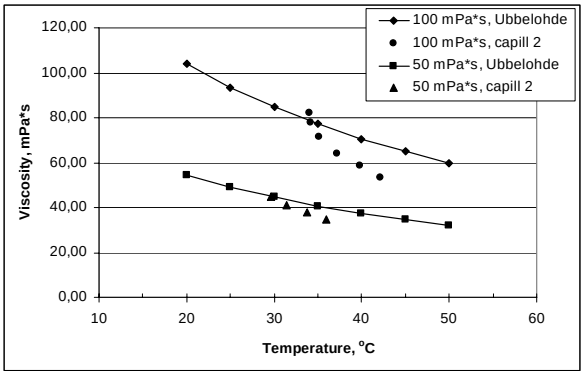

Fig. 4.2 Effect of temperature on viscosity of siloxane oils (50 and 100 mPa·s).

4.1.2 Measurements with SLIT

SLITs of three different lengths and five different heights (Table 3-2) were used. According to the theory, kinetic energy and Couette corrections were

applied to the results. Nevertheless, the oils demonstrated pronounced geometry dependent behaviour (Figs. 4.3 a-b).

The length-to-height ratio of the SLIT was found to affect the level of the oil's viscosity: an increase in the SLIT aspect ratio resulted in a decrease in the viscosity level. Furthermore, in certain ranges of the L/h ratio, the oils demonstrated similar levels of flow resistance. As the nearest approximation, these ranges can be named as follows: L/h>17; 11<L/h<17; 8<L/h<11; L/h<8 (Fig. 4.3).

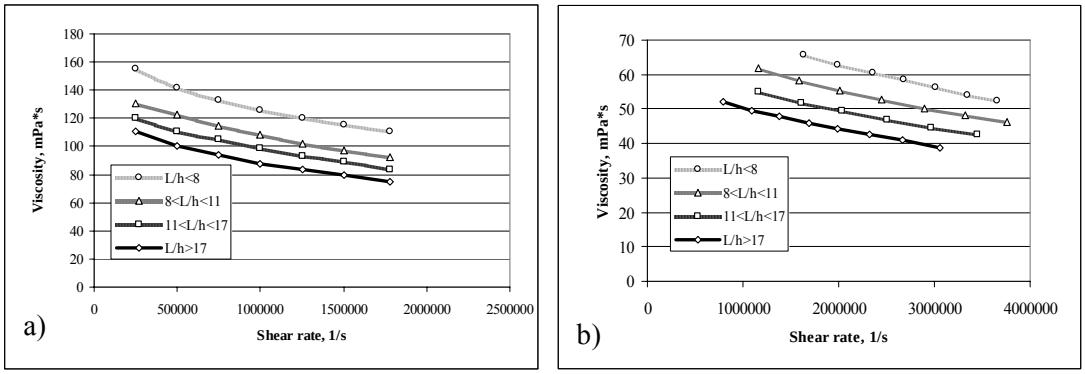

Fig. 4.3 High-shear viscosity of siloxane oil, **a)** 100 mPa·s and **b)** 50 mPa·s, measured with SLITs of different dimensions. Kinetic and Couette corrections are applied

Usually, geometry-dependent flow behaviour is observed when non-Newtonian viscoelastic fluids are measured with dies of different dimensions. However, this phenomenon is only observed with viscoelastic materials, while the L/h-dependent flow behaviour depicted in Fig. 4.3 was obtained in measurements of *inelastic* Newtonian materials. The possible reasons for this kind behaviour will be discussed further.

4.1.3 Comparison of capillaries and slit

Since Tsuji et al. /31/ also used silicone oil of standard viscosity 100 mPa·s in measurements with their Slit Die Rheometer (SDR), the SDR results were compared with those obtained with conventional capillaries and SLIT in the present study. Capillaries with L/d ratios of 112 and 152 as well as the SLIT belonging to the group L/h>17 were chosen for comparison with the results obtained with the SDR. The SDR slit had an aspect ratio of 140. To make the comparison possible, the same corrections as in Tsjui's study were applied to the data in the present study.

The results of the comparison are shown in Fig. 4.4. The viscosity of the fluid measured by Tsuji with SDR coincides with the results of the capillary measurements in the present study, whereas the viscosity shown by the SLIT is noticeably higher. Again, the clear effect of the aspect ratio can be noted: at a high aspect ratio, the capillary and slit flow of the Newtonian fluid appears to be independent of the dimensions and shape of the channel. The aspect ratios of the studied SLITs were in the range of 5.6 to 29.5, which seems small in comparison with the capillary L/d ratios.

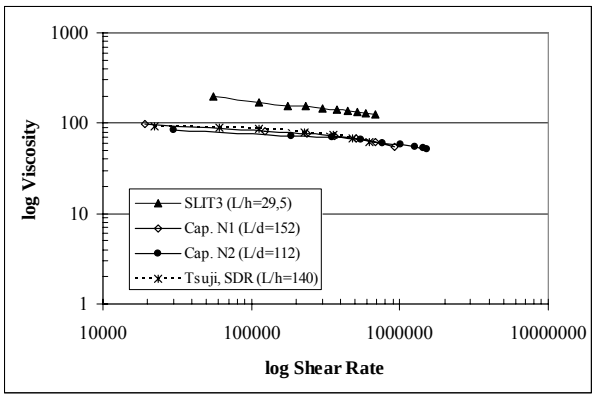

Fig. 4.4 Newtonian flow in the capillaries and SDR with high aspect ratio in comparison with small aspect ratio SLIT

4.2 Coating colours

4.2.1 Measurements with capillaries

Because of the end pressure losses, coating colours demonstrate geometry-dependent flow behaviour, i.e. different flow curves are obtained for different dimensions of the capillary (Fig. 4.5). The degree of entrance losses depends on the shear rate and properties of material measured. Thus, coating colours with more pronounced viscoelasticity give rise to a higher entrance pressure drop and more pronounced geometry dependence of uncorrected viscosity data. For instance, kaolin clay-based coating colours are known to have more elastic properties than calcium carbonate coatings.

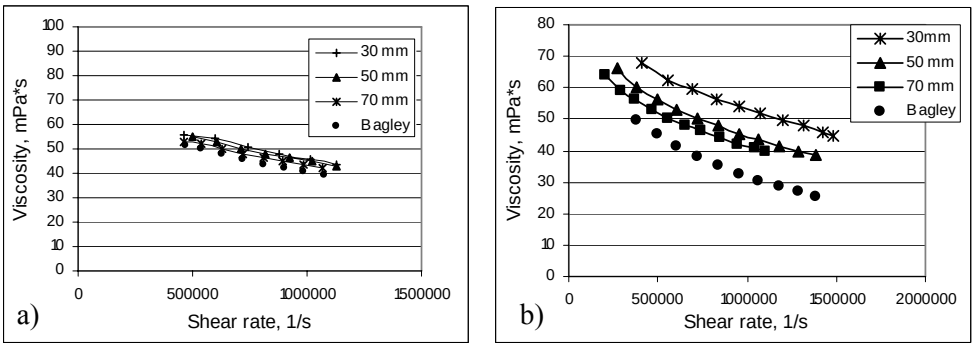

Fig. 4.5 Viscosity measured with capillaries (diameter 0.5mm, lengths 30, 50, and 70mm) and single viscosity curve after Bagley correction: **a)** HC90-based colour, 68% solids, **b)** SW80-based colour, 61.3% solids.

The Bagley plots obtained from the capillary measurements are shown in Fig. 4.6. As can be seen from the plots, the points for each flow rate are situated linearly, which means that end losses are independent of capillary length. After the entrance pressure losses were subtracted from the total pressure drop within each capillary, a single curve for viscosity, independent of tube length, was obtained (Fig. 4.5, filled circles).

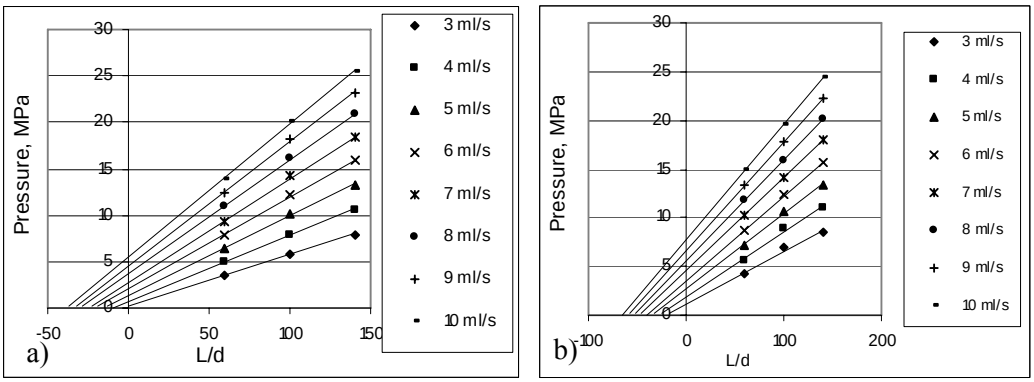

Fig. 4.6 Bagley plot for capillary measured coating colours **a)** HC90, **b)** SW80.

4.2.2 Measurements with SLIT

In the next step the same coating colours were measured with SLITs of three different lengths (0.5, 1.0, and 1.5mm). As can be seen from Fig. 4.7, the flow of coating colour shows almost the same trend in SLIT measurements as in the capillary ones: the flow resistance decreases with an increase in die length. One can also see the increased flow resistance in SLITs compared to

capillaries (Figs. 4.7 and 4.5). The kinetic energy and Couette corrections had been applied for the SLIT data.

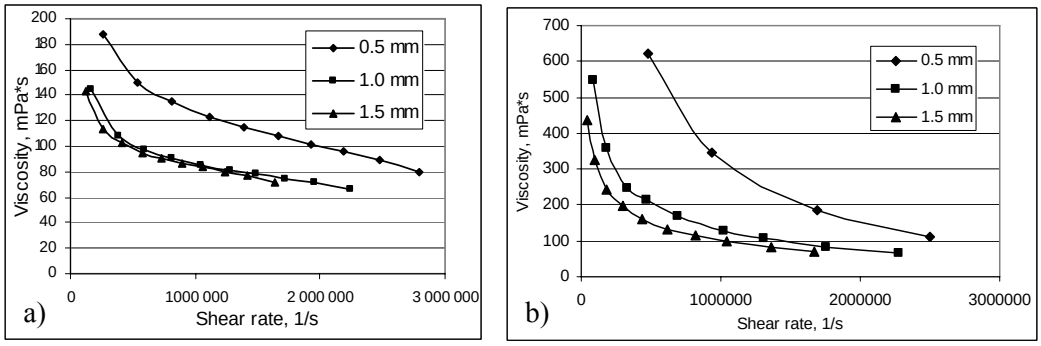

Fig. 4.7 Flow curves in the SLITs (length 0.5, 1.0, and 1.5mm: height 0.08mm): **a)** HC90, **b)** SW80

Assuming that the mechanism governing the SLIT flow is the same as that governing the capillary and that the end losses in the SLIT have the same origin as in the capillaries, application of the Bagley correction should result in the true viscosity curve, independent of the SLIT geometry.

For calcium carbonate, application of the Bagley correction resulted in typical linear relationship between total pressure and aspect ratio (Fig. 4.8 a). On the other hand, for kaolin clay, the Bagley plot demonstrated pronounced non-linearity (Fig. 4.8b), which was typical for all SLIT heights and for all kaolin-based coating colours.

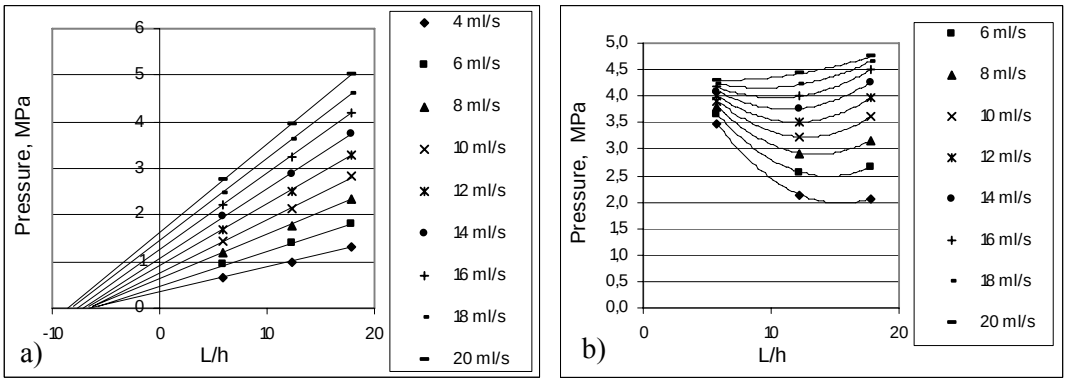

Fig. 4.8 Bagley plot for SLIT measured coating colours **a)** HC90, **b)** SW80

The concavity of the Bagley plot indicates that end losses in the SLIT are geometry-dependent: they increase with a decrease in the aspect ratio of the die. In this case, the correction for end effects cannot be applied to the results.

Since the Bagley plot for calcium carbonate looks typical and application of the Bagley method seems to be possible, the correction was applied to the SLIT data which were then compared to the similarly corrected capillary viscosity data. After the correction, the SLIT data did not result in a single viscosity curve, and the level of viscosity of the SLIT curves is still higher than those of the capillaries (Fig. 4.9).

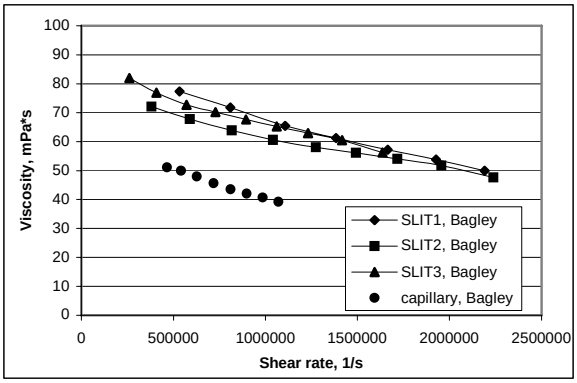

Fig. 4.9 Comparison of capillary and SLIT flow curves after Bagley correction.

4.3 Principles governing the flow through the SLIT

From the foregoing, the following observations should be distinguished:

- Geometry-dependent flow behaviour of Newtonian fluid (Figs. 4.3 a and b)
- Increased viscosity of Newtonian fluid and coating colour
- Geometry-dependence of the Bagley plot (for kaolin clay, Fig. 4.8 b)
- Bagley correction either gives incorrect viscosity values (for calcium carbonate, Fig. 4.9) or is not applicable (for kaolin clay, Fig. 4.8 b)

Han et al. have presented the theory of exit pressure loss /33, 34/. While the Bagley method takes into account the pressure drop both in the entrance and exit regions, the method suggested by Han separates entrance pressure losses and exit pressure losses from each other. According to Han, the entrance pressure drop depends only on the shear rate and properties of the measured material, while the exit pressure also varies with the aspect ratio of the tube /28, 33, 34, 39/. The exit pressure decreases rapidly as the aspect ratio increases, and beyond a certain critical value of the aspect ratio the exit pressure becomes negligible compared to the total applied pressure.

The flow of Newtonian fluids through small-aspect-ratio SLITs has been found to be highly dependent of the aspect ratio. This dependence was typical in the studied range of aspect ratios, i.e., 5.6-29.5. The viscosity of siloxane oils decreased with an increase in the L/h ratio, approaching to the capillary viscosity data. A further increase in the aspect ratio of the rectangular die resulted in viscosity data consistent with those for capillary measurements, i.e. the Newtonian flow became independent of the dimensions and shape of the measuring channel (Figs. 4.3 and 4.4). Therefore, it can be assumed that the flow through low-aspect-ratio SLITs is affected by a phenomenon of the same origin as the "exit pressure" effect demonstrated by viscoelastic materials.

Theoretically, it can be conceived that in high-aspect-ratio dies (capillary or slit) the flow profile becomes fully developed when a certain die length is reached. However, in low-aspect-ratio SLITs, the flow does not reach a steady state: disturbances caused by entrance effects prevail along the whole die length and in the exit region, causing an "exit pressure" effect, which is referred to as the residual entrance pressure loss (P_{res}). The presence of P_{res} causes a viscous pressure drop in the exit region, which is not taken into account in the procedure for Couette and kinetic corrections. In the same way as the exit pressure losses caused by the elasticity of the material decreases with an increase in the aspect ratio of the die /28, 33, 34, 39/, P_{res} (which has a viscous origin) is L/h-dependent.

Schematically, the pressure distribution in the SLIT can be presented as shown in Fig. 4.10.

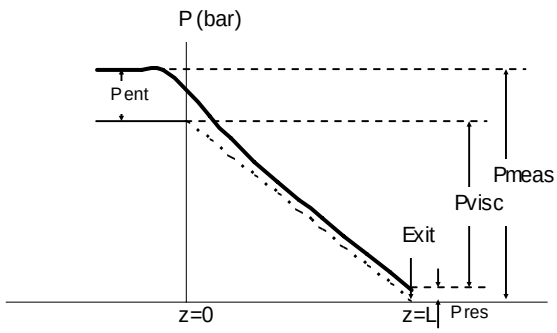

Fig. 4.10 Schematic diagram of the pressure distribution before and in the small L/h ratio SLIT (Newtonian fluid).

An increase in L/h, as the flow becomes more developed and approaches a steady state, causes the residual entrance pressure to decrease, thus leading to a decrease in viscosity (Fig. 4.11).

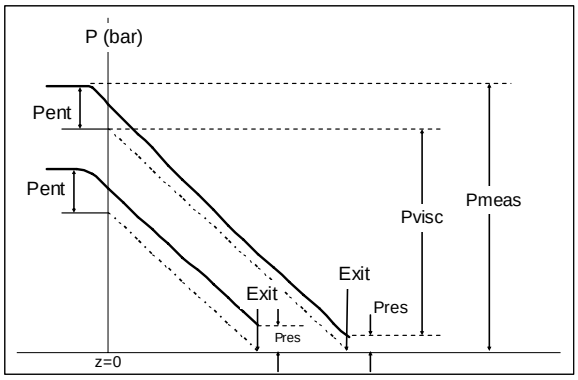

Fig. 4.11 Effect of die length on residual entrance pressure losses.

The main assumption of the Bagley method concerning the correction for end effects is that entrance pressure losses are not dependent on die geometry. Non-Newtonian viscoelastic fluids give rise to very much larger values of the entrance pressure drop (P_{ent}) than Newtonian fluids. The complex composition and viscoelastic and extensional properties of coating colours result in increased resistance to the converging flow at the die entrance, which is reflectes as an excessive entrance pressure loss /40/. Consequently, pressure losses at the exit from the SLIT are also higher. This is especially pronounced with kaolin clay-based coating colours due to their extensional properties and/or the increased flow resistance of the plate-like particles of kaolin. The geometry dependence of end losses is clearly seen from the concave Bagley plot. The total measured pressure increases with a decrease in the L/h ratio (Fig. 4.12).

Because of the presence of residual entrance pressure losses, the Bagley correction either gives erroneous results (Fig. 4.9, calcium carbonate) or is unapplicable (Fig. 4.8 b, kaolin clay). This is why in SLIT measurements flow resistance is preferred over real viscosity.

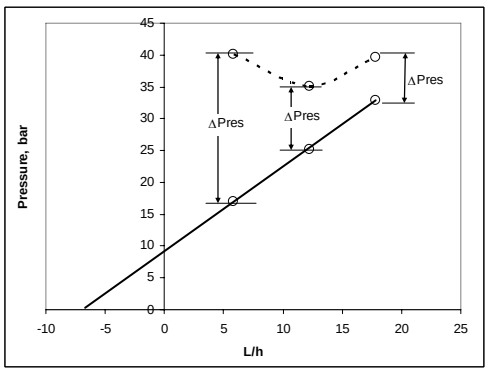

Fig. 4.12 Geometry dependence of total applied pressure in the SLIT (kaolin clay coating colour).

Based on the foregoing, the pressure distribution before and in the SLIT die can be schematically represented as shown in Fig. 4.13. For comparison, a schematic diagram of the pressure distribution in the capillary is shown in Fig.2.2.

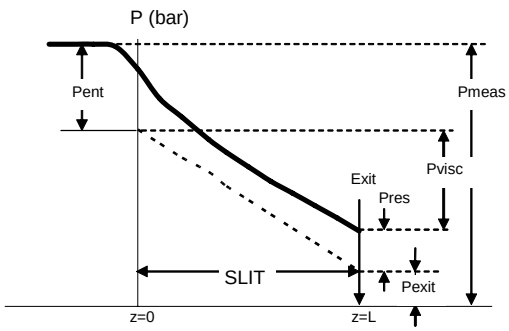

Fig. 4.13 Schematic diagram of pressure distribution before and in the SLIT. P_{ent} is a sum of P_{kin}, P_{Vent}, and P_{elast}.

The nature of the flow in the SLIT with low L/h is fundamentally different from that of conventional capillaries. In spite of the fact that true viscosity cannot be obtained with SLITs, the unstable flow in this kind of geometry suggests that SLITs might be better suited for simulating the unstable flow under the blade than commonly used capillary measurements.

4.4 Composition of coating colour and how it is characterised with the SLIT

This section describes how differences in the flow pattern of the capillary and SLIT affect the information provided by these geometries of the high-shear rheometer.

Effect of pigment grade

The pigments used in the measurements differed in their physical properties: particle shape, particle size distribution (PSD) and shape factor (Table 3-1). These are known to be among the most important factors affecting the rheology of coating colours in a wide range of shear rates. For instance,

diminishing particle size and/or narrowing particle size distribution leads to an increase in the viscosity of coating colours.

First, the capillary viscosity of all coating colours was adjusted to make it consistent. Consistent capillary (diameter 0.5 mm, length 50 mm) viscosity was achieved by varying the solids content of the colours (Table 3-1). Second, coating colours were measured with the SLIT in order to determine the effect of the geometry on their flow behaviour.

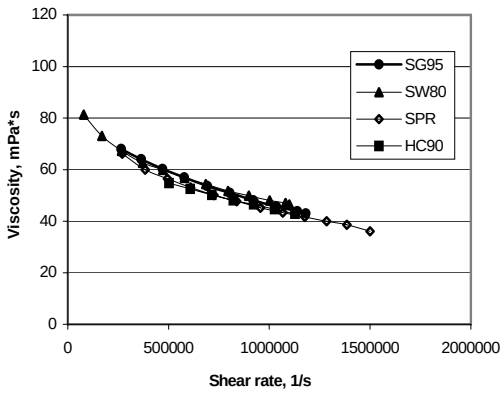

Fig. 4.14 a Viscosity of four coating colours measured with capillary (diameter 0.5 mm, length 50mm)

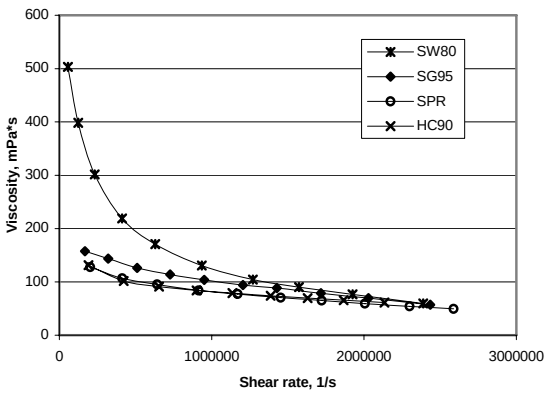

Fig. 4.14 b Viscosity of four coating colours measured with SLIT2 (height 0.09 mm, length 1.0 mm)

Despite the consistent capillary viscosity of all coating colours, there was a clear difference in their flow behaviour when measured with the SLIT (Figs. 4.14a and 4.14b). Calcium carbonate colour had a lower flow resistance than almost all kaolin-based coating colours; kaolin clay Suprawite80-based coating colour demonstrated the highest level of SLIT viscosity.

Differences in the flow behaviour of coating colours could have been caused by differences in viscoelastic properties and extensional properties only if the coating colours had contained different thickening agents. Since the same thickener was used in all coating colour formulations, it is doubtful that there was a significant difference in viscoelastic properties and extensional viscosities between the studied kaolin grades. The fact that the SLIT was able to differentiate between coating colours, whose viscosity was consistent in capillary measurements (Figs. 4.14a and 4.14b) could be explained by the greater dependence of the SLIT flow on pigment properties, i.e., particle shape, shape factor and PSD, and therefore the ability of particles to orientate and rearrange themselves in the flow channel.

Effect of thickeners

CMC molecules have been proven to form a network structure interacting with kaolin particles, provided that the coating colour is not subjected to deformations. As soon as deformation forces are applied, the network structure starts to break up. Therefore, colours based on clay demonstrate detectable resistance to shear, which is influenced by the amount and molecular weight of CMC added. It has also been shown /12/ that the polymer molecules of the thickener are not adsorbed onto particles of calcium carbonates, and no structure is formed between them. CMC molecules in this case stay in a liquid phase whose viscosity is influenced by the quantity and concentration of polymer molecules. Therefore, the flow resistance of carbonate-based colours is mostly influenced by the viscosity of the liquid phase and the rearrangement of particles in the flow /12/.

The next step in the study was to compare the capillary and SLIT flow behaviour of coating colours, when using two grades of CMC, one with low (CMC A) and the other with high (CMC B) molecular weight. Examples of the results are shown in Figs. 4.15a and 4.15b.

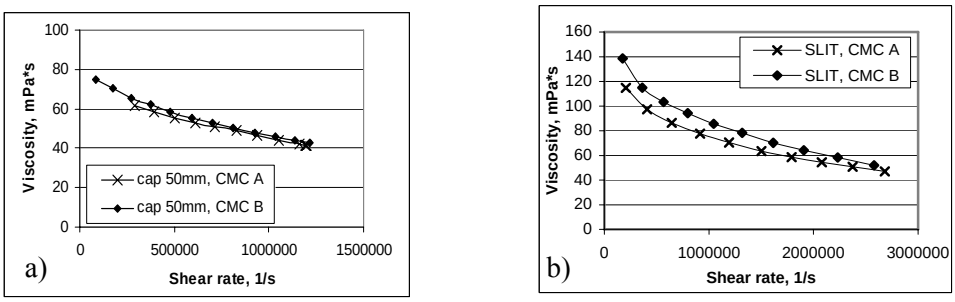

Fig. 4.15 Viscosity for SPR kaolin-based colour, 60% solids; **a)** Capillary (diameter 0.5mm, length 50mm) and **b)** SLIT2 (height 0.08mm, length 1.0mm)

The capillary viscosity of SPR-based coating colour depended to some extent on the molecular weight of the CMC used in the coating colour formulation (Fig. 4.15 a**)**. The effect of the CMC grade was even more prominent when performing the SLIT measurements: the decrease in SLIT flow resistance appeared to be more pronounced with low-molecular-weight CMC (Fig. 4.15 b). The capillary and the SLIT flow behaviour described above was also typical for calcium carbonate-based coating colour (see paper IV).

The flow behaviour of calcium carbonate-based colour was affected by the concentration of polymer molecules in the liquid phase, i.e. the molecular weight of CMC. The continuous-phase viscosity decreased when CMC with a lower molecular weight was used, which led to a decrease in the coating colour's viscosity.

When using CMC with lower molecular weight, the flow resistance of SPR-based colour also decreased. This might have been caused by a decrease in the forces required to break up of the network structure or by a decrease in the liquid-phase viscosity.

It might be concluded from the above that rearrangement of particles in the entrance region has a greater effect on the SLIT flow then on the capillary flow of coating colours.

4.5 Correlation to the coating process

Principle of correlation

In order to correlate the data obtained in high-shear rheological measurements with the coating process, laboratory coating trials were performed. For this purpose a Cylindrical Laboratory Coater (CLC-6000) was used.

The Cylindrical Laboratory Coater (CLC-6000) operates at commercial speeds and coat weights. The technique has been found to give reproducible blade loading results which correlate well with the viscosity at the shear rates that are the same as at commercial coaters although the blade loading and operation of the CLC is different from those of pilot and commercial coaters /41, 42/.
For each blade setting, different blade loads are applied and the blade position is adjusted to achieve the target coat weight /30/. Therefore, the monitored output data is the blade position at each trial point: higher blade loads correspond to smaller values of the blade position.

Figures 4.16a and b illustrate the blade position of the CLC required to achieve the target coat weights of 6 g/m^2 and 12 g/m^2, respectively, for the coating colours examined. As was to be expected, the blade distance needed to achieve a coat weight of 6 g/m^2 was smaller than that needed for the higher coat weight. Also, with increased machine speed, the blade distance needed

to control the target coat weight was reduced. It is also clear from the results that the studied coating colour formulations required a somewhat different blade position for coating with the target coat weights.

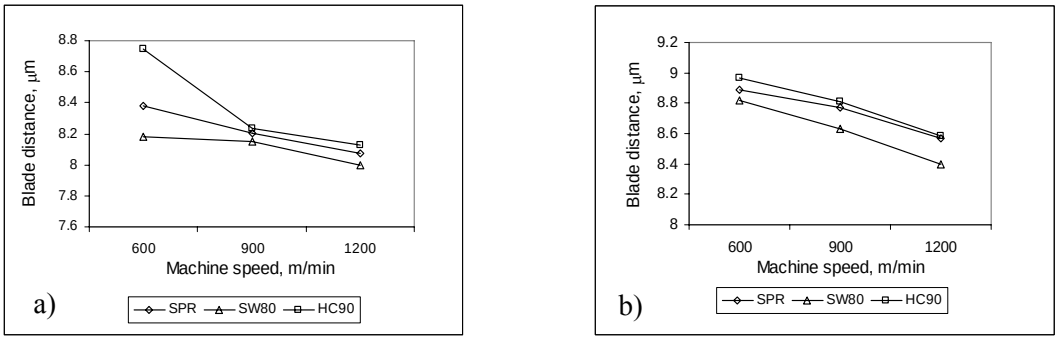

Fig. 4.16 Blade position vs. Coater speed **a)** for 6 g/m^2 coat weight and **b)** for 12 g/m^2 coat weight

To correlate coating run data with the results of rheological measurements, the shear rates which the coating colours are subjected to under the blade were estimated. For a given machine speed and target coat weight, shear rates were calculated by dividing the coater speed by the thickness of the coated layer. The latter was obtained according to Equation 4.5-1.

$$t = \frac{cw}{c \cdot \rho} \qquad \text{(Eq. 4.5-1)},$$

where t is the coated layer thickness, cw coat weight, c solids content of coating colour, and ρ density of coating colour.

For instance, the calculated shear rate for a machine speed of 600 m/min and a coat weight of 6 g/m^2 is about $7 \cdot 10^5 s^{-1}$. The share rate is roughly the same for the target coat weight of 12 g/m^2 when the machine is run at a speed of 1200 m/min.

The viscosity of coating colours obtained from rheological measurements at the shear rates corresponding to the given machine speed was then correlated to the recorded blade position of the CLC. Viscosity values were plotted on the X-axis and the blade position on the Y-axis. The degree of correlation was evaluated by comparing correlation coefficients and the general pattern of their changes depending on the impacting parameters.

Figures 4.17a and b show that in spite of their consistent capillary viscosity, the coating colours required different blade positions to achieve the target coat weights, which means that the correlation between the capillary viscosity and required blade positions is extremely poor or nonexistent.

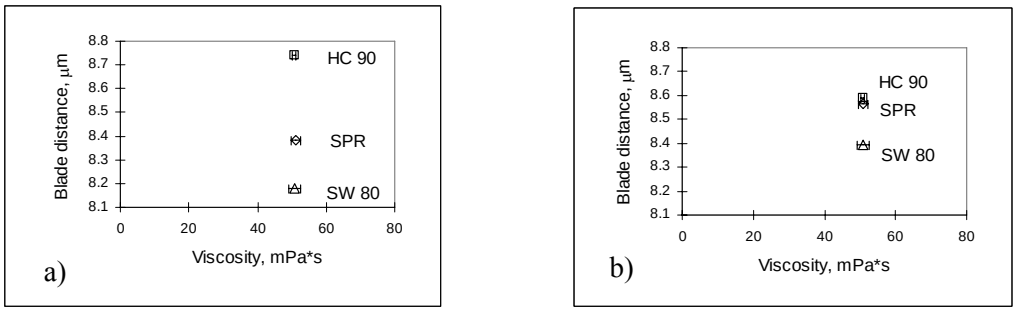

Fig. 4.17 Correlation of capillary viscosity (capillary №2) with blade position. **a)** Coat weight 6 g/m^2, coater speed 600 m/min, shear rate ~ $7 \cdot 10^5$ s^{-1}. **b)** Coat weight 12 g/m^2, coater speed 1200 m/min, shear rate ~ $7 \cdot 10^5$ s^{-1}.

The difference in blade position correlates quite well with the results of measurements made with the SLIT geometry of the high-shear rheometer. The coating colours, which demonstrated higher flow resistance in SLIT measurements, required a smaller blade distance to achieve the required coat weight (Figs. 4.18a and b). The depicted correlation was typical for SLITs of all studied dimensions (lengths and heights).

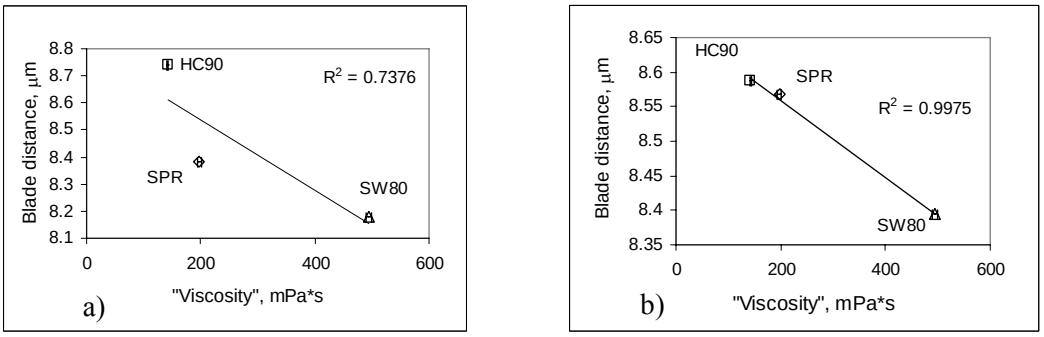

Fig. 4.18 Correlation of SLIT viscosity (SLIT1; length 0.5 mm, height 0.09 mm) with blade position **a)** coat weight 6 g/m^2, coater speed 600 m/min, shear rate ~$7 \cdot 10^5$ s^{-1}; **b)** coat weight 12 g/m^2, coater speed 1200 m/min, shear rate ~$7 \cdot 10^5$ s^{-1};

It is also known /43/ that entrance pressure losses in the capillaries can also be correlated with the blade loads. The entrance pressure losses in the capillary were calculated according to the procedure of Bagley correction

(see section 2.1.2); the obtained values were then used in the correlation with the blade distances instead of the viscosity data (Fig. 4.19).

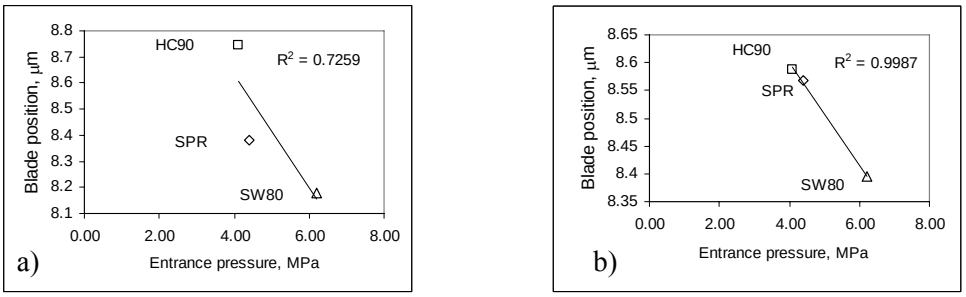

Fig. 4.19 a) Correlation of the entrance pressure drop in the capillary with blade position **a)** Coat weight 6 g/m^2, coater speed 600 m/min, shear rate ~ $7 \cdot 10^5$ s^{-1}. **b)** Coat weight 12 g/m^2, coater speed 1200 m/min, shear rate ~ $7 \cdot 10^5$ s^{-1}.

It can be seen that the calculated entrance pressure drops for the capillary data (Fig. 4.19) correlate with CLC blade positions as well as the SLIT data (Fig. 4.18). This demonstrates that the pressure loss effects occur during the coating. Furthermore, this once again demonstrates that the pressure loss effects govern the flow through the SLIT.

The good correlation of capillary data with the blade load can be obtained by using entrance pressure losses instead of the measured viscosity. The entrance pressure losses are determined by measurements with three capillaries differing in their length and further calculations by means of Bagley correction.

Effect of SLIT dimensions on correlation

Length

The flow through the SLIT was found to be unstable along the whole length of the die. The instability caused by entrance effects, referred to as residual entrance pressure loss, was still present at the exit from the SLIT. The losses were geometry-dependent, increasing with a decrease in the die aspect ratio, which leads to a decrease in the flow resistance of the coating colours.

Correlation of the rheological measurements with laboratory coating data demonstrated that an increase in die length impairs the correlation (Fig. 4-20 a-c). This tendency was observed for both target coat weights, with different SLIT heights and machine speeds. It should be noted here that SLIT 1 has the

dimensions closest to those of the blade nip, and according to the theory described in the foregoing, it is assumed to display greater flow instability.

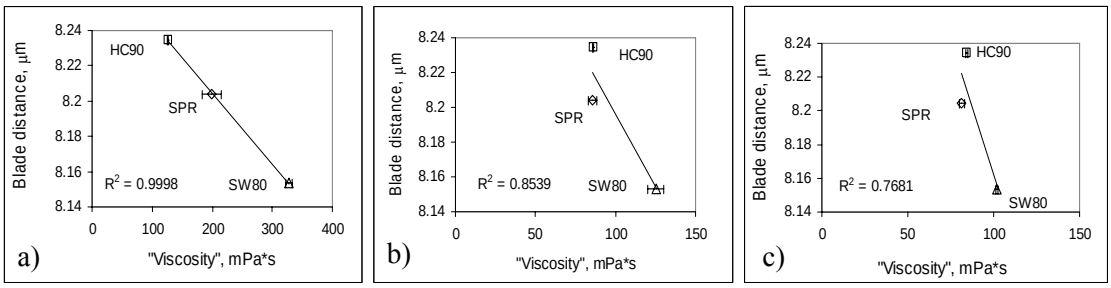

Fig. 4.20 Effect of SLIT length on correlation of CLC blade position with SLIT flow resistance (SLIT height 0.08 mm); coat weight 6g/m^2; machine speed 900 m/min: **a)** SLIT length 0.5 mm; **b)** SLIT length 1.0 mm; **c)** SLIT length 1.5 mm.

Height

As can be seen from Figure 4.21 a-c, height does not affect the correlation significantly, so the height of the SLIT die can be increased without any major effect on the prediction ability of the SLIT geometry. This might facilitate the measuring procedure, since practical experience has shown that too small height leads to blocking of the SLIT die by pigment particle aggregates, thus reducing the repeatability of the measurements and corrupting flow resistance data.

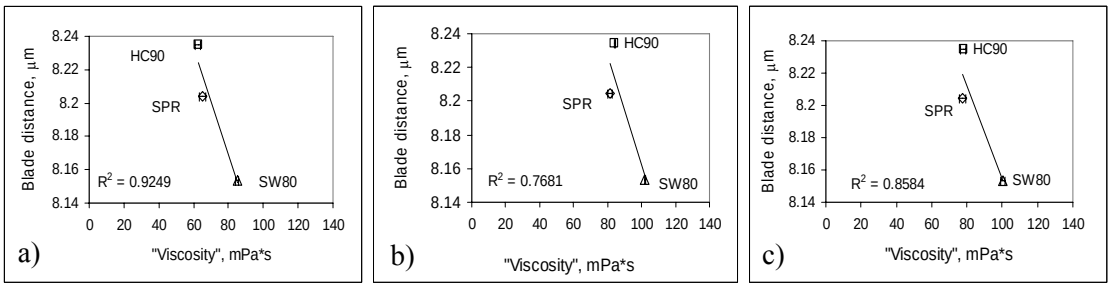

Fig. 4.21 Effect of SLIT height on correlation of CLC blade position with SLIT flow resistance (SLIT3; length 1.5 mm); coat weight 6g/m^2; machine speed 900 m/min: **a)** SLIT height 0.05 mm; **b)** SLIT height 0.08 mm; **c)** SLIT height 0.09 mm.

Effect of coater speed and coat weight

The effect of coater speed on the correlation of the blade position with the SLIT flow resistance was analysed. The estimated shear rates for the machine speeds of 600, 900 and 1200 m/min and a coat weight of 12 g/m^2 were $3 \cdot 10^5$, $5 \cdot 10^5$, and $7 \cdot 10^5$ s^{-1}, respectively. An increase in coater speed slightly improves the degree of correlation with the SLIT measurement results.

The correlation of the CLC blade position with the SLIT flow resistance of coating colours appeared to be slightly better at the higher coat weight. This dependence was observed for all studied sets of the SLITs' dimensions. The poorer correlation at the lower coat weight can be explained by theoretical considerations related to the force balance under the blade and differences in coat weight control at high and low coat weight. At low coat weight, the blade position is more sensitive to the characteristics of the base paper than at high coat weights.

5 CONCLUSIONS

The objectives of the study were to determine the factors affecting the flow behaviour of coating colours, to compare the information given by this type of rheometry with that obtained with the conventional capillary technique, and to evaluate the ability of the SLIT to predict the relationship between coat weight and blade pressure.

It was found that the flow through the SLIT does not attain a fully developed velocity profile and is unstable along the whole length of the SLIT. The instability caused by entrance effects is present at the exit from the SLIT as residual entrance pressure (P_{res}). In case of a Newtonian flow, only viscous effects cause residual entrance pressure losses.

The residual entrance pressure is L/h-dependent: an increase in L/h, as the flow approaches steady state, causes P_{res} to decrease, thus leading to a decrease in the viscosity level. At the critical die length, when flow instabilities are overcome, P_{res} becomes equal to zero.

The principle of the flow through the SLIT die differs from that of traditional capillary viscometry. Because of this difference, SLIT rheometry is more sensitive to particle shape, particle size distribution and the type of thickener used in the coating colour formulation than the capillary method.

In a laboratory trial with a Cylindrical Laboratory Coater, the differences in coating formulations reflected by the SLIT measurements were found to be in good correlation with the blade position required to achieve the target coat weights. Coating colours, which demonstrated higher flow resistance in SLIT measurements, required a smaller blade distance to achieve the required coat weight. The correlation was best for the shortest SLIT with a length of 0.05 mm, which is close to the geometry of the blade tip.

The height of the SLIT was found to be insignificant for the degree of correlation, which means that the height of the die can be increased to at least 0.09 mm to facilitate the measurement procedure without impairing the prediction ability of the rheometer geometry.

The results obtained in this study are fairly promising with a view to the prediction ability of the SLIT geometry of a high-shear rheometer in comparison to conventional capillary measurement.

Nevertheless, it seems to be important for future exploitation of the SLIT to collect more knowledge on this type of high-shear rheometry. It would be useful to perform further study with extended selection of coating colour formulations, where more components are varied like thickeners, latexes, etc. where the SLIT data would be verified on either a pilot coating scale or even a mill scale.

It also should be noted that the limitations characterising the SLIT rheometry are the same as for conventional capillary measurement. Neither method takes into account all the phenomena occurring under the blade, such as the back flow of coating colour, coating colour dewatering, properties of the base paper etc. Therefore, SLIT rheometry should not be considered as a direct simulator of the blade levelling process. However, in view of the sensitivity of the SLIT geometry to the composition of the coating colour, as well as its ability to predict the blade loads needed to achieve target coat weights, SLIT rheometry might be helpful in developing new coating colour formulations and can therefore be considered as a useful tool for research purposes.

LITERATURE

1. **Ghosh, T.,** "Rheology of Kaolin-based Pigment Slurries and the Coating Colors They Form: Part II", Tappi J. 81(5):123-126 (1998)
2. **Ching, B.,** "The Characteristics of Engineered Kaolin Pigments and Its Applications in LWC Paper Coatings", TAPPI Coating Conference, Dallas, p. 419-424 (1995)
3. **Alince, B., Lepoutre, P.,** "Flow Behavior of Pigment Blends", TAPPI Coating Conference, San Francisco, p. 201-206 (1983)
4. **Eklund, D.,** "Pigment Particle Size – Its Significance in Paper Coating", Cellulose Chemistry and Technology, 9(3):299-312 (1975)
5. **Grön, J., Dahlvik, P.,** "Influence of Pigment Particle Characteristics on Coating Colour Properties", Paperi ja Puu, 78(9):533-540 (1996)
6. **Bousfield, D.W.,** "Particle Motion During Shear. The influence of particle shape and roughness on rheology", Nordic Pulp Paper Res. J., 8(1):176-183 (1993)
7. **Triantafillopoulos, N.G.,** "Paper Coating Viscoelasticity and Its Significance in Blade Coating", TAPPI Press, Atlanta, 1996, 80 pp.
8. **Schempp, W., Friesen, W., Klapp, H., Lederer, K., Schurz, J.,** "Characterization of Clay suspensions by High Shear Rate Viscometry, Zeta-Potential Measurements and Small Angle X-Ray Scattering", Cellulose Chemistry and Technology, 10(1):89 (1976)
9. **Fadat, G., and Rigdahl, M**., "Viscoelastic Properties of CMC/Latex Coating Colors", Nordic Pulp Paper Res. J., (1):30 (1987)
10. **Davis, R.M.,** "The Colloidal Chemistry of CMC-Latex Coatings", Tappi J., 70(5):99-105 (1987)
11. **Oittinen, P.,** "The Interactions between Coating Pigments and Soluble Binders in Dispersions", TAPPI Coating Conference, Houston, p. 113-122 (1981)
12. **Grön, J., Kuni, S.,** "The Impact of Different Coating Pigments and Molecular Weight of Carboxy Methyl Cellulose on Coating Structure", TAPPI Coating Conference, Dallas, p. 447-457 (1995)
13. **Ghosh, T., Carreau, P., J., Lavoie, P-A.,** "Rheology of Coating Colors and their Runnability on a Cylindrical Laboratory Coater", TAPPI Coating Conference, Nashville, p. 303-308 (1996)
14. **Windle, W. and Beazley, K.M.,** "The Mechanics of Blade Coating", Tappi, 50(1):1-7 (1967)
15. **Yannas, J.B. and Gonzales, R.N.,** "Low Shear Viscometry in the Prediction of Coating Performance", Tappi, 45(2):156-159 (1962)
16. **Lehtinen, E;** Editor, "Papermaking Science and Technology, Book 11: Pigment Coating and Surface Sizing of Paper", Chapters 5.6, 24.1.3.2, and 31.1,, Fapet Oy/TAPPI Press, 2000, 810 pp.
17. **Kahila, S.J., Eklund, D.E.,** "Factors influencing the coat weight in blade coating with beveled blade – theory and practice. In proc.", TAPPI Coating Conference, Atlanta, p. 13-29 (1978)

18. **Gane, P.A.C., Watters, P.,** "Pigment Particle Orientation", Paperi ja Puu, 71(5):517-533 (1989)

19. **Gane, P.A.C., Watters, P., McGenity, P.M.,** "Factors Influencing the Runnability of Coating Colours at High Speed", TAPPI Coating Conference, Orlando, p. 117-132 (1992)

20. **Purkayastha, A., Oja, M.E.,** "Dynamic Rheological Behavior of Paper Coatings", TAPPI Advanced Coating Fundamentals Symposium, Minneapolis, p. 31-41 (1993)

21. **Roper III, J.A., Attal, J.F.,** "Evaluations of Coating High-Speed Runnability Using Pilot Coater Data, Rheological Measurements, and Computer Modeling", Tappi J., 76(5):55-61 (1993)

22. **Ziler, Z., Bousfield, W.,** "The Motion of Disk-Shaped Pigments in Transient Shear Flows", TAPPI Coating Conference, Orlando, p. 373-384 (1992)

23. **Whalen-Shaw, M., Gautam, N.,** "A model for the colloidal and rheological characteristics of clay-latex-CMC formulations", Tappi Coating Conference, Boston, p. 371-385 (1990)

24. **Young, T.S., Fu, E.,** "Associative behaviour of cellulosic thickeners and its implications on coating structure and rheology", Tappi J., April 1991, 74(4):197-207 (1991)

25. **Engström, G., Rigdahl, M.,** "The Implication of Viscoelasticity on Coating Rheology and Structure", Tappi J., 70(5):91 (1987)

26. **Grankvist, T.O., Såndas, S.E.**, "Measurement of viscoelasticity at low and high shear rates", TAPPI Coating Conference, Boston, p. 473-478 (1990)

27. **Carreau, P.J., Lavoie, P-A.,** "Rheology of coating colours: a rheologist point of view", TAPPI Advanced Coating Fundamentals Symposium, Minneapolis, p. 1-12 (1993)

28. **Han, C. D.**, "Rheology in Polymer processing", Academic press, New York-San Francisco-London, 1976, 357 pp.

29. **Lodge, A. S., Ko, Y.-S.,** "Slit die viscometry at shear rates up to $5x10^6$ s^{-1}: an analytical correction for small viscous heating errors", Rheological Acta, 28:464-472 (1989).

30. **Ramthun, J., Reif, L., Wallpott, G., Rahlwes, D.**, "A New Laboratory Method for Predicting the Runnability of a Coating Mix "On a High Speed Coater", TAPPI Coating Conference, Chicago, p. 27-35 (1989)

31. **Tsuj, A., Sasagawa, Y.**, "A New Rheometer for Paper Coating", TAPPI Coating Conference, Boston, p. 453-458 (1990)

32. **Mäkinen, M., Egorova, N., Happonen, J., Lehtinen, E., Laine, J.E.**, "Using slit viscometers to predict coating perfomance on high speed Coaters", Paper Technology, 42(9):30-34 (2001)

33. **Han, C. D., Charles, M., Philippoff, W.,** "Rheological Implications of the Exit Pressure and Die Swell in Steady Capillary Flow of Polymer Melts. I. The Primary Normal Stress Difference and the Effect of L/D Ratio on Elastic Properties", J. Rheol., 14(3):393-408 (1970)

34. **Han, C. D., Charles, M.,** "Entrance- and Exit-Correction in Capillary Flow of Molten Polymers", J. Rheol., 15(2):371-384 (1971)

35. **Bagley, E. B.**, "End corrections in the Capillary Flow of Polyethylene", J. Appl. Physics, 28(5):624-627 (1957)

36. **Lohmander, S., To, A.**, "Rheological characterisation of coating colours – comparison between conventional techniques and a slit die system", Nordic Pulp Paper Res. J., 16 (2):88-95 (2001)

37. **Husband, J.C., Tran, D.,** "A study of formulation effects on ultra high shear viscosity of coating colours measured with a slit die", 5th International Paper and Coating Symposium 2003, p. 85-91 (2003)

38. **Lehtinen, E.,** "Effect of pigment packing on rheology of coating colour and structure of coating", Pigmentit paperin raaka-aineena 1998-2001 teknologiaohjelman loppuraportti, TEKES, Helsinki 2002, pp.80-85 (2002)

39. **Han, C.D.**, "Note: On the Use of the Bagley Plot", J. Rheol., 17(2):375-383 (1973)

40. **Willenbacher, N., Hanciogullari, H.,** "Analysis of coating colour runnability considering the effect of dewatering. Part1: Apparent wall slip and viscoelasticity at high shear rates", TAPPI advanced coating fundamentals Symposium, p.1-8 (1997)

41. **Guler, E., Bousfield, D.W.,** "Blade force measurements on a laboratory puddle coater", TAPPI Coating Conference, Dallas, p. 53-65 (1995)

42. **Mohan, R., Scheller, B.L.,** "Effect of Dispersed Phase Solids on Blade Forces in Cylindrical Laboratory Coater", J. Pulp Paper Sci., 27(2):54-59 (2001)

43. **Wilson, T.S., Greenbladt, G.D.,** "Capillary viscometry of paper coating colors and correlation to coating behavior", Polymeric Materials Science and Engineering, 73:484-485 (1995)